

Probing CP-violating Higgs-gauge Boson Couplings at Future Muon Collider

Emre Gurkanli^{*1} and Serdar Spor^{†2}

¹*Department of Physics, Sinop University, Türkiye.*

²*Department of Medical Imaging Techniques,*

Zonguldak Bülent Ecevit University, 67100, Zonguldak, Türkiye.

(Dated: November 8, 2024)

Abstract

We explore the sensitivity of future muon colliders to CP-violating interactions in the Higgs sector, specifically focusing on the process $\mu^-\mu^+ \rightarrow h\bar{\nu}_l\nu_l$. Using a model-independent approach within the framework of the Standard Model Effective Field Theory (SMEFT), we analyze the contribution of dimension-six operators to Higgs-gauge boson couplings, emphasizing CP-violating effects. To simulate the process, all signal and background events are generated through MadGraph. The analysis provides 95% confidence level limits on the relevant Wilson coefficients \tilde{c}_{HB} , \tilde{c}_{HW} , \tilde{c}_γ , with a comparative discussion of existing experimental and phenomenological constraints. Our best constraints on the \tilde{c}_{HB} , \tilde{c}_{HW} , \tilde{c}_γ with an integrated luminosity of 10 ab^{-1} are $[-0.017148; 0.018711]$, $[-0.002545; 0.002837]$ and $[-0.010613; 0.011210]$, respectively. In this context, this study highlights the capability of future muon collider experiments to probe new physics in the Higgs sector, potentially offering tighter constraints on CP-violating Higgs-gauge boson interactions than those provided by current colliders.

PACS numbers: 14.80.Ec, 14.70.Hp

Keywords: Neutral Higgs Bosons, Models beyond the Standard Model.

^{*} egurkanli@sinop.edu.tr

[†] serdar.spor@beun.edu.tr

I. INTRODUCTION

The discovery of the 125 GeV Higgs boson by the ATLAS [1] and CMS [2] collaborations at the Large Hadron Collider (LHC) marked a turning point in our understanding of fundamental physics, confirming the Higgs mechanism as responsible for electroweak symmetry breaking (EWSB). This discovery was a key validation of the Standard Model (SM), yet it also opened new questions about the deeper nature of the Higgs boson. While the current experimental data align well with the SM predictions, particularly indicating that the Higgs is a CP-even scalar [3–7], the matter-antimatter asymmetry observed in the universe suggests there may be new, unexplored sources of CP violation [8–10].

In the SM, CP violation occurs primarily through the Cabibbo-Kobayashi-Maskawa (CKM) matrix in weak interactions [11, 12]. However, the level of CP violation it provides is insufficient to explain the baryon asymmetry of the universe, indicating that additional mechanisms must exist beyond the SM [13]. This motivates the exploration of Higgs boson interactions with gauge bosons and fermions, which could harbor new CP-violating effects. These interactions, if discovered, could provide key insights into the origin of the universe’s matter dominance and guide us towards a more complete theory of particle physics [14].

One of the most promising frameworks for investigating these interactions is the Standard Model Effective Field Theory (SMEFT). By incorporating higher-dimensional operators, SMEFT allows for the systematic study of potential new physics contributions to Higgs couplings. In particular, CP-violating operators that couple the Higgs boson to gauge boson pairs (such as $HZ\gamma$, HZZ and HWW) are of special interest. Precision measurements of these couplings could reveal deviations from SM predictions, pointing towards new physics.

Future high-energy colliders like the future muon collider are poised to make significant contributions in this area. With its ability to probe Higgs boson properties with unparalleled precision at multiple energy stages, the muon collider offers a unique opportunity to explore both CP-conserving and CP-violating interactions. By conducting detailed studies on the Higgs boson’s couplings with SM particles, the muon collider could potentially provide the experimental evidence for new sources of CP violation, offering a crucial key to solving the puzzle of the matter-antimatter asymmetry and leading to discoveries beyond the SM.

This study, therefore, focuses on exploring the potential CP-violating Higgs-gauge boson couplings using dimension-six operators within the SMEFT framework, and outlines the

significance of these investigations in future collider experiments. In the following, after introducing our theoretical framework for the CP-violating Higgs-gauge boson couplings (Sec. II), we will present our strategy for testing for CP-violating Higgs-gauge boson couplings at the future muon collider in Sec. III, and our results in Sec. IV. Finally, we offer our conclusions in Sec. V.

II. EFFECTIVE THEORY APPROACH

Effective field theory (EFT) is a model-independent approach that simply analyzes deviations from the SM to study the properties of the Higgs boson. In this approach, new physics contributions beyond the SM, in addition to the SM Lagrangian, are parameterized as higher-dimensional operators. The effective Lagrangian respects the $SU(3)_C \times SU(2)_L \times U(1)_Y$ gauge symmetries, and the operators can be constrained separately by the Wilson coefficients as free parameters.

We consider the interactions of the Higgs boson and electroweak gauge bosons in the Strongly Interacting Light Higgs (SILH) basis [15]. If the effects of physics beyond the SM are described by the dimension-six operators \mathcal{O}_i , the effective Lagrangian is given by:

$$\mathcal{L} = \mathcal{L}_{\text{SM}} + \sum_i \bar{c}_i \mathcal{O}_i = \mathcal{L}_{\text{SM}} + \mathcal{L}_{\text{CPV}} \quad (1)$$

where \bar{c}_i are dimensionless Wilson coefficients normalized by the form of the new physics scale Λ identified with the W -boson mass m_W and \mathcal{L}_{SM} is the dimension-four SM Lagrangian. In this paper, we focus on the CP-violating interactions of the Higgs and electroweak gauge bosons, and these are written in terms of the SILH basis:

$$\mathcal{L}_{\text{CPV}} = \frac{ig\tilde{c}_{HW}}{m_W^2} D^\mu \Phi^\dagger T_{2k} D^\nu \Phi \widetilde{W}_{\mu\nu}^k + \frac{ig'\tilde{c}_{HB}}{m_W^2} D^\mu \Phi^\dagger D^\nu \Phi \widetilde{B}_{\mu\nu} + \frac{g'^2 \tilde{c}_\gamma}{m_W^2} \Phi^\dagger \Phi B_{\mu\nu} \widetilde{B}^{\mu\nu} \quad (2)$$

where $T_{2k} = \sigma_k/2$ with σ_k is the Pauli matrices. $B_{\mu\nu} = \partial_\mu B_\nu - \partial_\nu B_\mu$ and $W_{\mu\nu}^k = \partial_\mu W_\nu^k - \partial_\nu W_\mu^k + g\epsilon_{ij}^k W_\mu^i W_\nu^j$ are the field strength tensors corresponding to $U(1)_Y$ and $SU(2)_L$ of the SM gauge groups, respectively, with gauge coupling constants g' and g . $\widetilde{B}_{\mu\nu} = \frac{1}{2}\epsilon_{\mu\nu\rho\sigma} B^{\rho\sigma}$ and $\widetilde{W}_{\mu\nu}^k = \frac{1}{2}\epsilon_{\mu\nu\rho\sigma} W^{\rho\sigma k}$ are the dual field strength tensors. D^μ is covariant derivative operator and Φ is the Higgs doublet in the SM.

An effective Lagrangian in the mass basis with anomalous Higgs couplings is used for a phenomenological and experimental approach. It has proven to be a useful approach to relate experimental bounds expressed in terms of anomalous couplings to phenomenological bounds obtained by theories or models. The relevant subset of anomalous $HZ\gamma$, HZZ and HWW couplings in the mass basis and in the unitary gauge is written as [16]:

$$\mathcal{L} = -\frac{1}{4}\tilde{g}_{hzz}Z_{\mu\nu}\tilde{Z}^{\mu\nu}h - \frac{1}{2}\tilde{g}_{h\gamma z}Z_{\mu\nu}\tilde{F}^{\mu\nu}h - \frac{1}{2}\tilde{g}_{hww}W^{\mu\nu}\tilde{W}_{\mu\nu}^\dagger h \quad (3)$$

where h is Higgs boson field. The relation between these anomalous coupling coefficients in the mass basis and the dimension-six coefficients are given by:

$$\tilde{g}_{hzz} = \frac{2g}{c_W^2 m_W} [\tilde{c}_{HB} s_W^2 - 4\tilde{c}_\gamma s_W^4 + c_W^2 \tilde{c}_{HW}] \quad (4)$$

$$\tilde{g}_{h\gamma z} = \frac{gs_W}{c_W m_W} [\tilde{c}_{HW} - \tilde{c}_{HB} + 8\tilde{c}_\gamma s_W^2] \quad (5)$$

$$\tilde{g}_{hww} = \frac{2g}{m_W} \tilde{c}_{HW} \quad (6)$$

where $s_W = \sin\theta_W$ and $c_W = \cos\theta_W$ with θ_W being the weak mixing angle. There are three Wilson coefficients, \tilde{c}_{HB} , \tilde{c}_{HW} and \tilde{c}_γ for CP-violating couplings.

We focus on the sensitivity study of \tilde{c}_{HB} , \tilde{c}_{HW} and \tilde{c}_γ coefficients in the anomalous $HZ\gamma$, HZZ and HWW vertices through the $\mu^-\mu^+ \rightarrow h\bar{\nu}_l\nu_l$ process with single Higgs boson production at the muon collider, and the investigation of the CP-violating properties of the anomalous couplings. In this paper, analysis of the dimension-six operators in Higgs-gauge boson couplings are performed into `MADGRAPH5_aMC@NLO` [17] based on Monte Carlo simulations using `FeynRules` [18] and the `UFO` [19] framework. The `HEL` model file [16] containing the 39 dimension-six operators and their corresponding Wilson coefficients is implemented in `FeynRules`.

There are many phenomenological studies to obtain constraints on the Wilson coefficients of CP-conserving and/or CP-violating dimension-six operators using various channels at the pp [20–26], ee [27–34], ep [35, 36] and $\mu\mu$ [37] colliders. Focusing on the design of

a muon collider with high luminosity and high energy, the International Muon Collider Collaboration (IMCC) [38] has recently been studying the possibility of developing a muon collider with 10 TeV center-of-mass energy. In this study, we consider a 10 TeV center-of-mass energy ($\sqrt{s} = 10$ TeV) muon collider that produces an integrated luminosity equal to 10 ab^{-1} per interaction point (IP). Lepton colliders are generally known to have much smaller backgrounds and a cleaner environment than hadron colliders. Because muons are 207 times heavier than electrons, muon collisions produce less synchrotron radiation than electron-positron collisions, making it easier to accelerate them to high energies with a circular collider. Muon colliders, which have the advantage of both being lepton collider and operating at multi-TeV energies, offer a unique opportunity in the search for new physics by enabling precise measurements of Higgs-gauge bosons couplings.

The Feynman diagrams of the $\mu^-\mu^+ \rightarrow h\bar{\nu}_l\nu_l$ process including the anomalous Higgs-gauge bosons vertices are given in Fig. 1. These Feynman diagrams represent signal processes involving new physics contributions from the anomalous $HZ\gamma$, HZZ and HWW vertices.

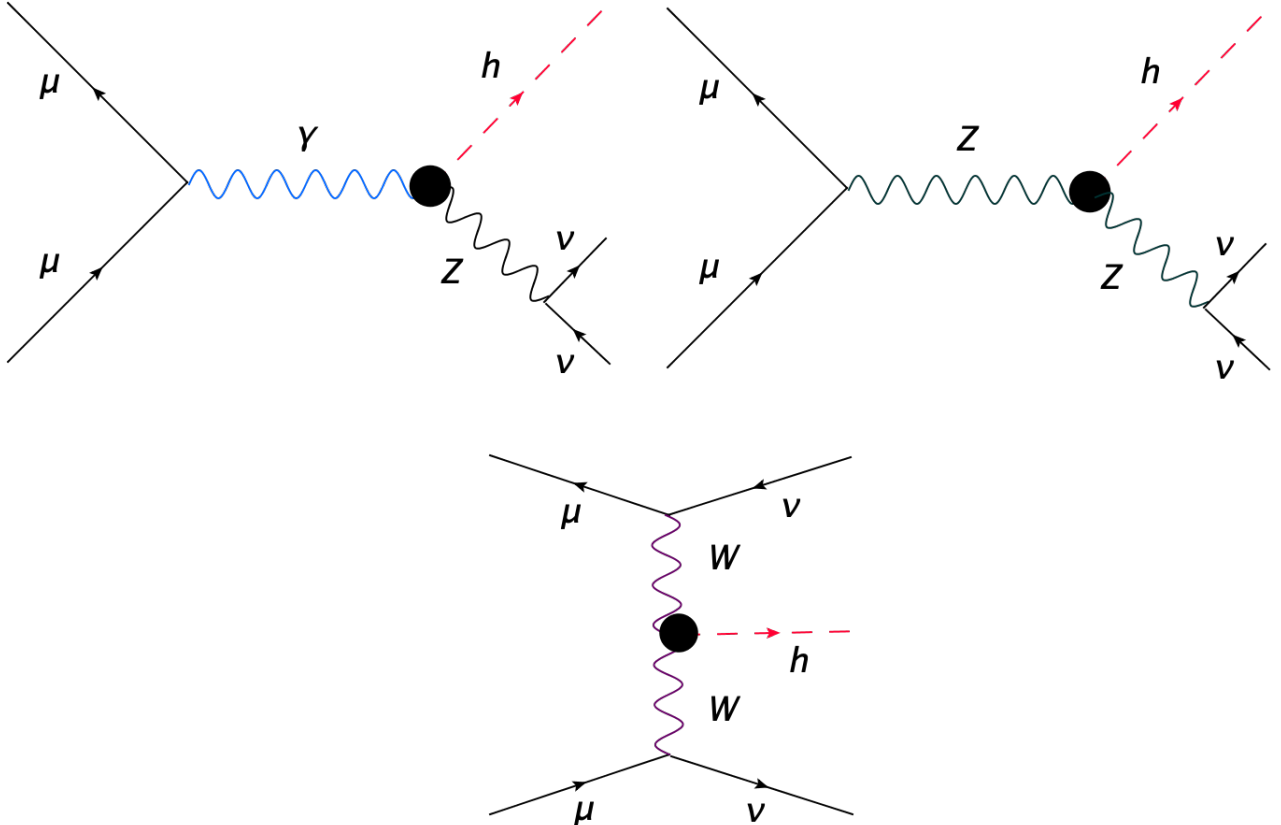


FIG. 1: Feynman diagrams of the $\mu^-\mu^+ \rightarrow h\bar{\nu}_l\nu_l$ process including the anomalous Higgs-gauge bosons vertices.

The total cross-sections of the process $\mu^-\mu^+ \rightarrow h\bar{\nu}_l\nu_l$ in term of coefficients \tilde{c}_{HB} , \tilde{c}_{HW} and \tilde{c}_γ at the muon collider are shown in Fig. 2. The calculation method of the total cross-sections in Fig. 2 is that a certain coefficient is variable each time, while the other coefficients are fixed to zero. All Wilson coefficients being equal to zero ($\tilde{c}_{HB} = \tilde{c}_{HW} = \tilde{c}_\gamma = 0$) correspond to the cross-section of the SM contribution in the process $\mu^-\mu^+ \rightarrow h\bar{\nu}_l\nu_l$.

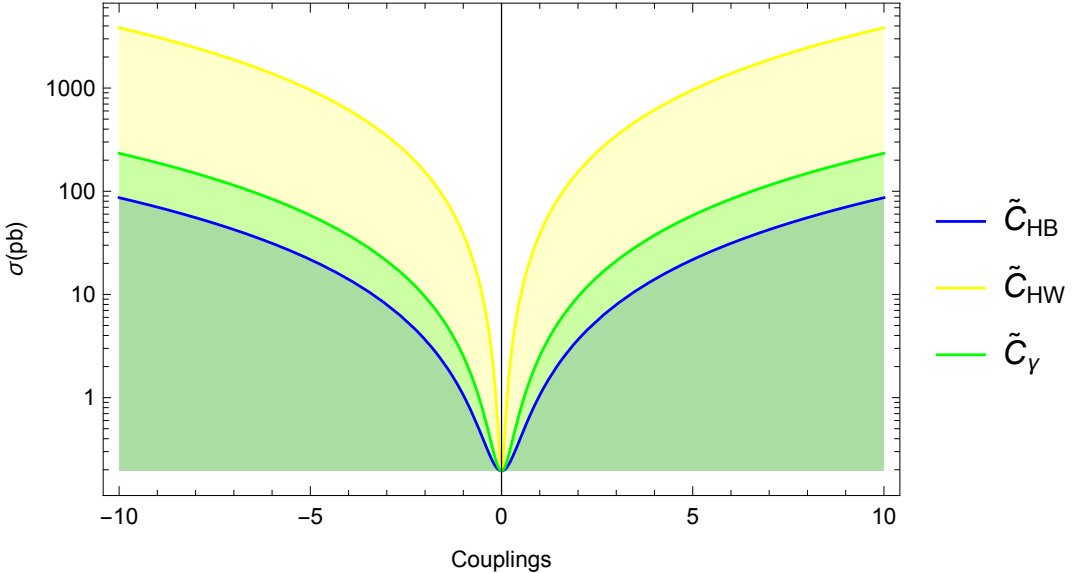


FIG. 2: The total cross-sections of the process $\mu^-\mu^+ \rightarrow h\bar{\nu}_l\nu_l$ in terms of the coefficients \tilde{c}_{HB} , \tilde{c}_{HW} and \tilde{c}_γ at the muon collider.

III. EVENT GENERATION AND CUT-BASED ANALYSIS

In this section, we describe our simulation setup and apply a cut-based analysis to derive constraints on anomalous $HZ\gamma$, HZZ and HWW Higgs-gauge boson couplings via the process $\mu^-\mu^+ \rightarrow h\bar{\nu}_l\nu_l$ at the muon collider. The process $\mu^-\mu^+ \rightarrow h\bar{\nu}_l\nu_l$ serves as signal, including SM contributions, pure new physics terms with contributions from non-zero coefficients \tilde{c}_{HB} , \tilde{c}_{HW} , \tilde{c}_γ and the interference terms between the SM and pure new physics terms. On the other hand, a series of background processes are examined to have a more realistic simulation. Each background process is defined as follows: the $B_{H\nu\nu}$ represents the SM background the process $\mu^-\mu^+ \rightarrow h\bar{\nu}_l\nu_l \rightarrow b\bar{b}\bar{\nu}_l\nu_l$, which has the same final state as the signal process. The following other backgrounds are: i) the process $\mu^-\mu^+ \rightarrow Z\bar{\nu}_l\nu_l \rightarrow b\bar{b}\bar{\nu}_l\nu_l$ is labeled as $B_{Z\nu\nu}$, considering that one Z -boson decays to $b\bar{b}$. ii) the pair production of top

quark is realized through the process $\mu^-\mu^+ \rightarrow t\bar{t} \rightarrow W^+bW^-\bar{b} \rightarrow \ell^+\nu_l b\ell^-\bar{\nu}_l\bar{b}$ labeling as $B_{t\bar{t}}$, where one top quark (anti-top quark) decays to W^+b ($W^-\bar{b}$) which contains the leptonic decay channel of the W^\pm -boson. iii) the Z -boson pair production is labeled as B_{ZZ} and taken into account via the process $\mu^-\mu^+ \rightarrow ZZ \rightarrow b\bar{b}\bar{\nu}_l\nu_l$ where one Z -boson decays to $b\bar{b}$ and the other Z -boson decays to $\nu_l\bar{\nu}_l$.

To simulate signals for each coupling and relevant backgrounds, we generated 400 k samples using `MADGRAPH5_aMC@NLO`. For signal identification, a set of cuts was applied to separate signal and backgrounds in the $b\bar{b}\nu\nu$ final state. First the transverse momentum distributions for the final state b-quark for signal and relevant background processes at muon collider are presented in Fig. 3. It can be seen from Fig. 3 that the signal can be separated from the backgrounds by $p_T^b > 50$ GeV. Fig. 4 shows pseudo-rapidity distributions for b-quark, with a distinct separation in signal occurring for $|\eta^b| < 2.4$, which is implemented as Cut-1.

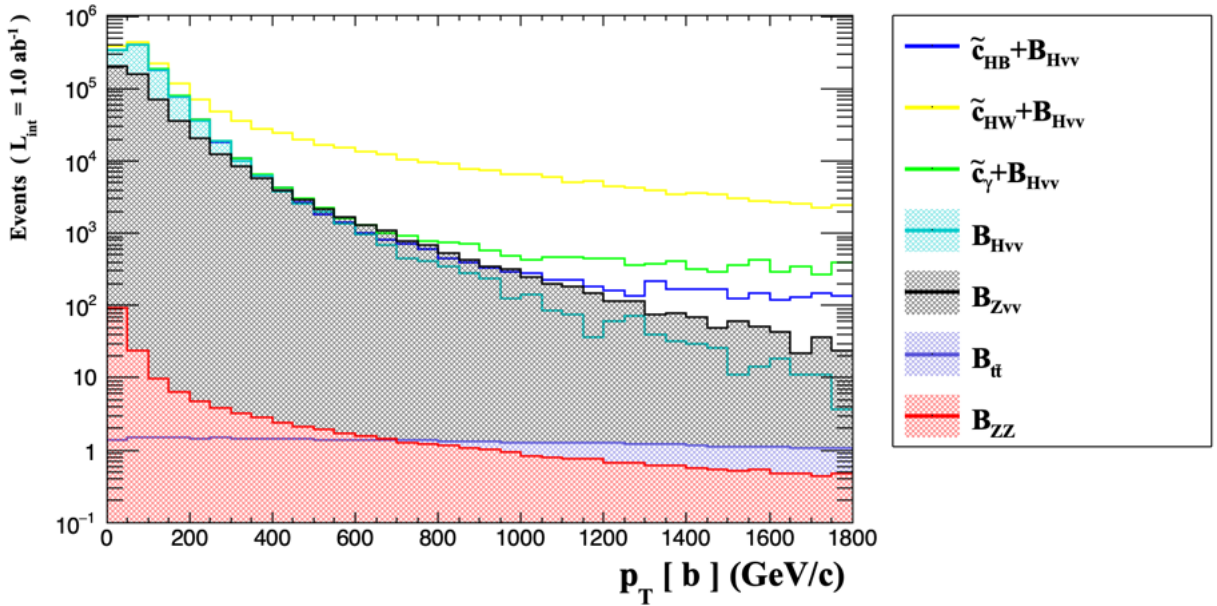


FIG. 3: The number of events as a function of p_T^b for the process $\mu^-\mu^+ \rightarrow h\bar{\nu}_l\nu_l$ and related backgrounds at muon collider with $\sqrt{s} = 10$ TeV.

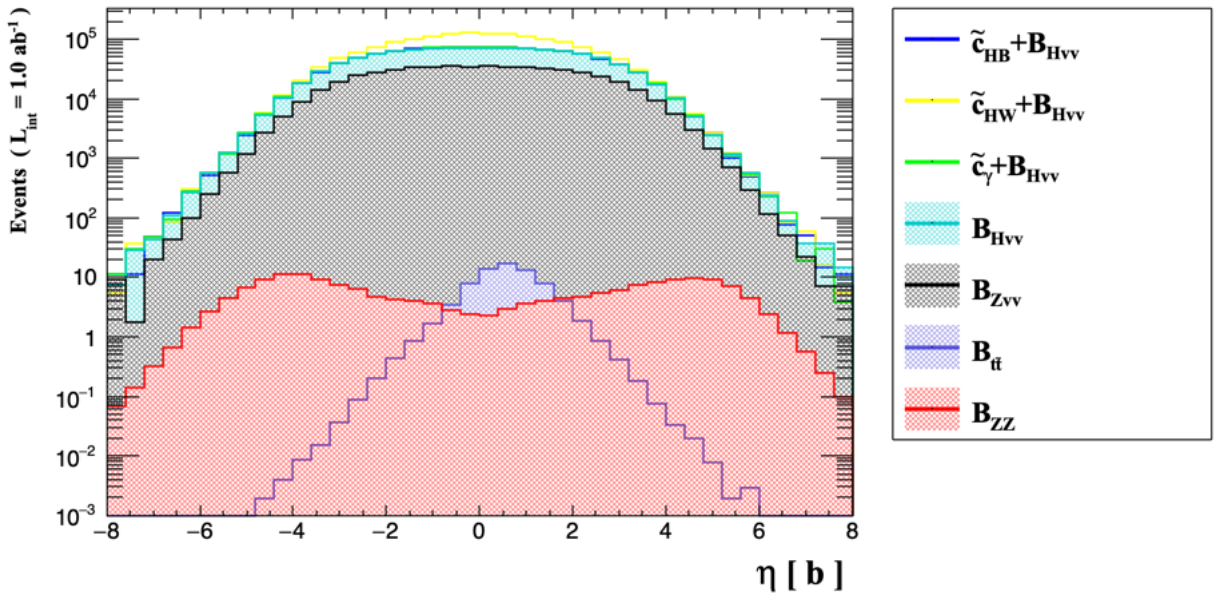


FIG. 4: The number of events as a function of η^b for the process $\mu^-\mu^+ \rightarrow h\bar{\nu}_l\nu_l$ and related backgrounds at muon collider with $\sqrt{s} = 10$ TeV.

On the other hand, Fig. 5 and Fig. 6 demonstrate that background suppression is further achieved by imposing missing transverse energy $\cancel{E}_T > 100$ (Cut-2) and restricting the distance between final state b-quarks $\Delta R(b, \bar{b}) < 1.6$ (Cut-3).

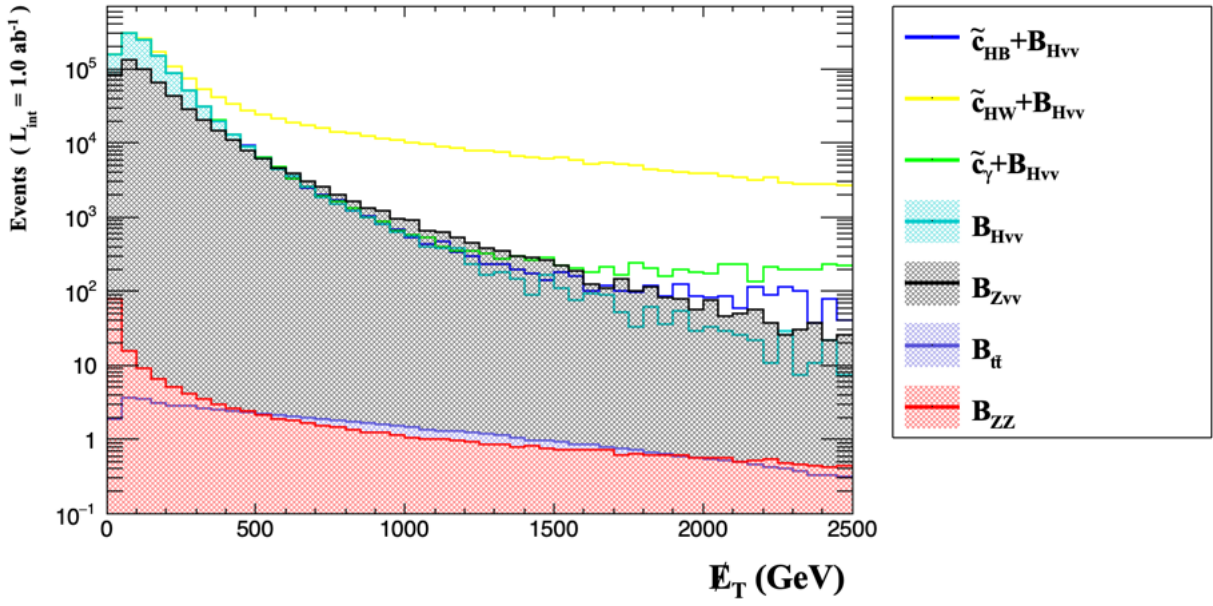


FIG. 5: The number of events as a function of \not{E}_T for the process $\mu^-\mu^+ \rightarrow h\nu_l\nu_l$ and related backgrounds at muon collider with $\sqrt{s} = 10$ TeV.

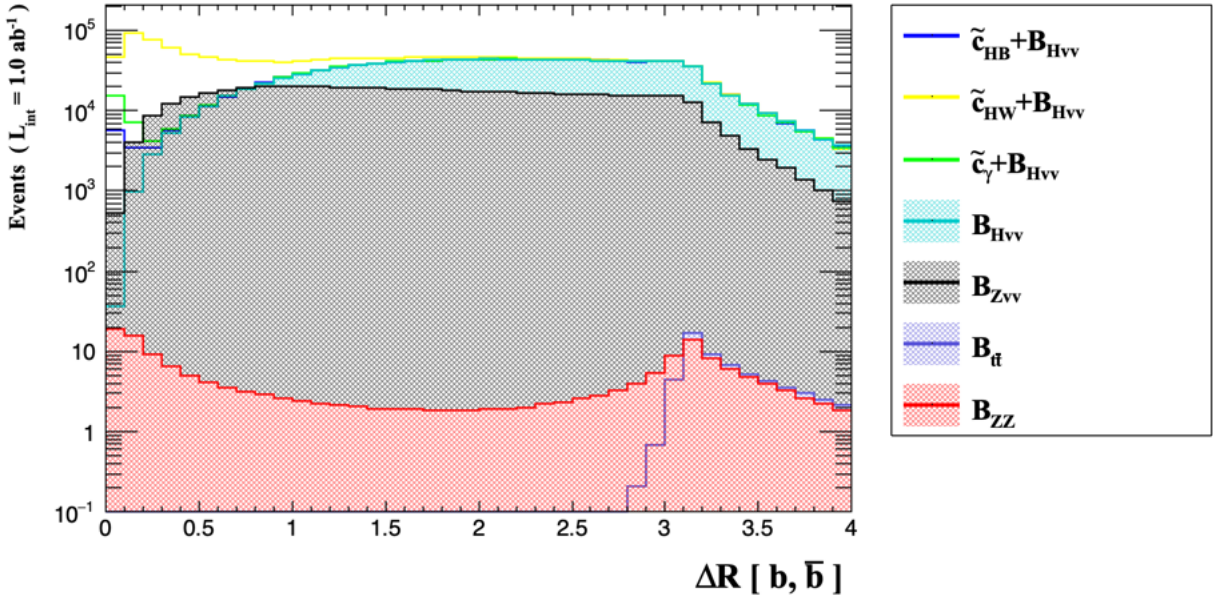


FIG. 6: The number of events as a function of $\Delta R_{b\bar{b}}$ for the process $\mu^-\mu^+ \rightarrow h\nu_l\nu_l$ and related backgrounds at muon collider with $\sqrt{s} = 10$ TeV.

For the invariant mass of the final state b-quarks from the decay of the Higgs boson, shown in Fig. 7, we set $120 < M_{b\bar{b}} < 130$ GeV (Cut-4).

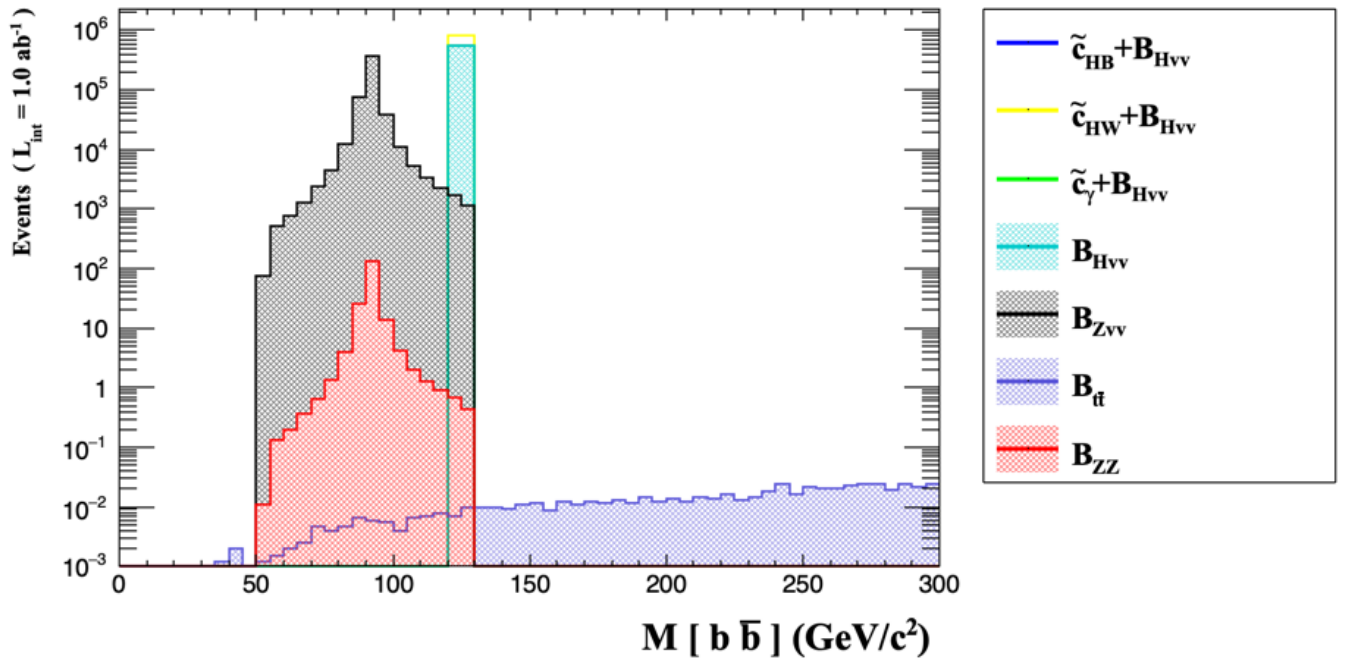


FIG. 7: The number of events as a function of $M_{b\bar{b}}$ for the process $\mu^-\mu^+ \rightarrow h\bar{\nu}_l\nu_l$ and related backgrounds at muon collider with $\sqrt{s} = 10$ TeV.

Finally, the list of particle-level cuts that are used in our calculations are given in a flow in Table I. On the other hand, Table II shows the number of events after each cut for the signals ($\tilde{c}_{HB} = 0.1$, $\tilde{c}_{HW} = 0.1$, $\tilde{c}_\gamma = 0.1$) and relevant backgrounds ($B_{H\nu\nu}$, $B_{Z\nu\nu}$, $B_{t\bar{t}}$, B_{ZZ}). The number of events are calculated with an integrated luminosity of $\mathcal{L}_{\text{int}} = 1 \text{ ab}^{-1}$ for each cut of the signal and relevant backgrounds. As seen in Table II, Cut-4 shows a significant improvement for enhancing separation between the signals and related backgrounds.

TABLE I: Particle-level selection cuts for the $\mu^-\mu^+ \rightarrow h\bar{\nu}_l\nu_l$ signal at the muon collider.

Kinematic Cuts		\tilde{c}_{HB} , \tilde{c}_{HW} , \tilde{c}_γ
Cut-1		$p_T^b > 50$, $ \eta^b < 2.4$
Cut-2		$\cancel{E}_T > 100$ GeV
Cut-3		$\Delta R(b, \bar{b}) < 1.6$
Cut-4		$120 < M_{b\bar{b}} < 130$ GeV

TABLE II: The number of events of Higgs-gauge boson couplings for the process $\mu^-\mu^+ \rightarrow h\bar{\nu}_l\nu_l$ and relevant backgrounds. Here, $\epsilon[\%]$ is the relative efficiency of each cut and $M = 10^6$.

MuCol.	Presel.		Cut-1		Cut-2		Cut-3		Cut-4	
Signal	Events	$\epsilon[\%]$	Events	$\epsilon[\%]$	Events	$\epsilon[\%]$	Events	$\epsilon[\%]$	Events	$\epsilon[\%]$
$\tilde{c}_{HB} = 0.1$	1.10M	—	0.57M	52	0.39M	68	0.25M	64	0.25M	100
$\tilde{c}_{HW} = 0.1$	1.61M	—	0.99M	61	0.81M	82	0.66M	81	0.66M	100
$\tilde{c}_\gamma = 0.1$	1.12M	—	0.58M	52	0.40M	69	0.27M	68	0.27M	100
Backgrounds										
$B_{h\bar{\nu}_l\nu_l}$	1.09M	—	0.56M	51	0.38M	68	0.24M	63	0.24M	100
$B_{Z\bar{\nu}_l\nu_l}$	0.54M	—	0.25M	46	0.19M	76	0.16M	84	868	0.005
$B_{t\bar{t}}$	73	—	71	97	66	93	0	0	0	0
B_{ZZ}	186	—	42	23	42	100	42	100	0	0

IV. EXPECTED SENSITIVITIES ON DIM-6 CP-VIOLATING HIGGS-GAUGE BOSON COUPLINGS

The sensitivities of dimension-six Higgs-gauge boson interactions to anomalous couplings was examined using simulated data from muon collisions at a center-of-mass energy of 10 TeV. The analysis was conducted using a χ^2 test to quantify the deviations from SM predictions. This test compares the total cross-section, including contributions from effective couplings, with the cross-section of backgrounds. Both systematic and statistical uncertainties were considered to obtain accurate error margins. The χ^2 test is defined as follows:

$$\chi^2(\tilde{c}_{HB}, \tilde{c}_{HW}, \tilde{c}_\gamma) = \left(\frac{\sigma_{SM}(\sqrt{s}) - \sigma_{Total}(\sqrt{s}, \tilde{c}_{HB}, \tilde{c}_{HW}, \tilde{c}_\gamma)}{\sigma_B(\sqrt{s}) \sqrt{(\delta_{sys})^2 + (\delta_{st})^2}} \right)^2, \quad (7)$$

Here, $\sigma_{SM}(\sqrt{s})$ represents the cross-section of the SM background, and $\sigma_{total}(\sqrt{s}, \tilde{c}_{HB}, \tilde{c}_{HW}, \tilde{c}_\gamma)$ is the total cross-section of both the new physics coming from beyond the SM and the SM background. On the other hand, $\sigma_B(\sqrt{s})$ is the total background that we consider in the analysis. $\delta_{st} = \frac{1}{\sqrt{N_B}}$ and δ_{sys} are the statistical error and

systematic uncertainty, respectively. The event number of the SM background is defined as $N_B = \mathcal{L} \times \sigma_B$, where \mathcal{L} is the integrated luminosity.

The primary focus of the analysis was to obtain the sensitivities on various Higgs-gauge boson couplings with the at 95% Confidence Level (C.L.). Systematic errors were accounted for in the calculations to reflect more realistic experimental conditions. Here, possible sources of systematic uncertainties are integrated luminosities, photon efficiencies, jet-photon misidentification, detector efficiency and background estimation. The obtained sensitivities on Higgs-gauge couplings at 95% C.L. are given in Table III under the systematic uncertainties of 0%, 3% and 5% and compared with the experimental results.

TABLE III: Sensitivities at 95% C.L. on the anomalous Higgs-gauge boson couplings for various systematic uncertainties.

		Muon Collider	
Effective Couplings	Experimental Results (ATLAS)	Systematic Errors	Our Projection
\tilde{c}_{HB}	$[-0.23; 0.23]$ [39]	$\delta = 0\%$	$[-0.017148; 0.018711]$
	$[-0.16; 0.16]$ [40]	$\delta = 3\%$	$[-0.115928; 0.117490]$
	$[-0.065; 0.063]$ [41]	$\delta = 5\%$	$[-0.149875; 0.151437]$
\tilde{c}_{HW}	$[-0.23; 0.23]$ [39]	$\delta = 0\%$	$[-0.002545; 0.002837]$
	$[-0.16; 0.16]$ [40]	$\delta = 3\%$	$[-0.017361; 0.017652]$
	$[-0.065; 0.063]$ [41]	$\delta = 5\%$	$[-0.022453; 0.022744]$
\tilde{c}_γ	$[-0.0018; 0.0018]$ [39]	$\delta = 0\%$	$[-0.010613; 0.011210]$
	$[-0.00028; 0.00043]$ [41]	$\delta = 3\%$	$[-0.070770; 0.071367]$
		$\delta = 5\%$	$[-0.091442; 0.092039]$

The results in Table III indicate that our projections provide particularly strong sensitivity to deviations from the SM, with the limits on the \tilde{c}_{HB} , \tilde{c}_{HW} couplings being highly constrained at 10 TeV muon collider with integrated luminosities of 10 ab^{-1} comparing with the ATLAS results.



FIG. 8: Comparison of ATLAS bounds and obtained sensitivities on the anomalous \tilde{c}_{HB} , \tilde{c}_{HW} , \tilde{c}_γ parameters via the process $\mu^-\mu^+ \rightarrow h\bar{\nu}_l\nu_l$ at muon collider.

On the other hand, Fig. 8 compare the obtained sensitivities at future muon collider and the experimental results for ATLAS results with barcharts [40, 41]. As seen in Fig. 8 our results demonstrates the potential of future muon colliders to probe new physics scenarios with unprecedented precision. Finally, to evaluate how constraints on a specific CP-violating coupling are affected by the presence of others, two-dimensional contours are considered in which the other coefficient is fixed at zero while scanning is performed on these two Wilson coefficients. Fig. 9 illustrates the 95% C.L. contours in the $\tilde{c}_{HB}-\tilde{c}_{HW}$, $\tilde{c}_{HB}-\tilde{c}_\gamma$, and $\tilde{c}_\gamma-\tilde{c}_{HW}$ planes, based on a two-parameter analysis at muon collider for the systematic uncertainties of 0%, 3% and 5%.

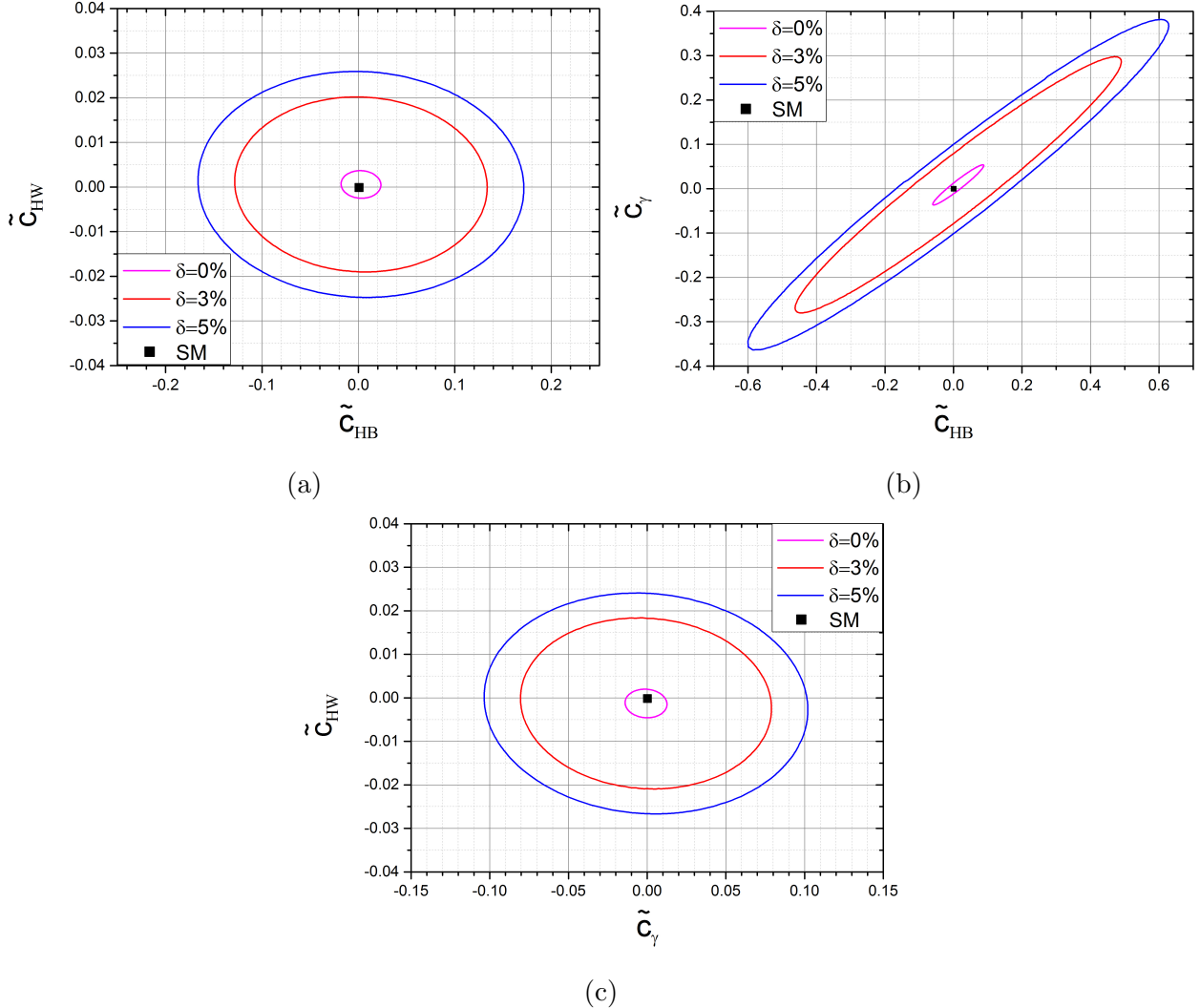


FIG. 9: Two-dimensional 95% C.L. intervals in plane for $\tilde{c}_{HB} - \tilde{c}_{HW}$ (a), $\tilde{c}_{HB} - \tilde{c}_\gamma$ (b) and $\tilde{c}_\gamma - \tilde{c}_{HW}$ (c) with taking systematic error $\delta_{sys} = 0\%, 3\%$ and 5% at the muon collider. The black square dot symbol represents the SM expectation.

V. CONCLUSIONS

We have investigated the sensitivity of CP-violating dimension-6 operators in the Higgs-gauge boson sector using the process $\mu^-\mu^+ \rightarrow h\bar{\nu}_l\nu_l$ at a future muon collider with $\sqrt{s} = 10$ TeV and an integrated luminosity of 10 ab^{-1} . Our analysis, which included a detailed study of kinematic distributions such as the transverse momentum, pseudo-rapidity and the ΔR of the final state b quarks, missing energy transverse and the invariant mass of the Higgs boson, aimed to provide new limits on the Wilson coefficients \tilde{c}_{HB} , \tilde{c}_{HW} , and \tilde{c}_γ .

The obtained sensitivity limits at 95% C.L. for these parameters are $[-0.017148; 0.018711]$, $[-0.002545; 0.002837]$, and $[-0.010613; 0.011210]$, respectively. When compared to the experimental limits of $[-0.23; 0.23]$ [39], $[-0.16; 0.16]$ [40] and $[-0.065; 0.063]$ [41] for both \tilde{c}_{HB} and \tilde{c}_{HW} , and $[-0.00028; 0.00043]$ [41] for \tilde{c}_γ , we observe a significant improvement in the constraints on the \tilde{c}_{HB} and \tilde{c}_{HW} couplings. However, for \tilde{c}_γ , while our results do not surpass the experimental limits provided by ATLAS at $\sqrt{s} = 13$ TeV with an integrated luminosity of 139 fb^{-1} , they still offer valuable insights that are consistent with phenomenological study at CLIC and muon collider in Ref. [37]. Our results, combined with muon collider's clean experimental environment, the high center-of-mass energy and integrated luminosities, make it a highly promising platform to probe new physics beyond the SM and this is the main motivation for designing this study at future muon collider.

In conclusion, our study demonstrates that future muon colliders, operating at $\sqrt{s} = 10$ TeV with high integrated luminosity, will play a crucial role in advancing our understanding of the Higgs sector, particularly in scenarios involving CP-violating Higgs-gauge boson interactions. The enhanced sensitivity to \tilde{c}_{HB} and \tilde{c}_{HW} couplings, along with competitive results for \tilde{c}_γ , underscores the potential of such colliders to explore physics beyond the SM. Future experiments at lepton colliders, combined with complementary results from hadron colliders, will provide a comprehensive approach to probing the fundamental nature of Higgs-gauge boson interactions and their possible CP-violating extensions.

VI. DATA AVAILABILITY STATEMENT

This manuscript has no associated data or the data will not be deposited. [Authors' comment: Data will be made available upon reasonable request.]

- [1] G. Aad *et al.* [ATLAS Collaboration], *Phys. Lett. B* **716**, 1-29 (2012).
- [2] S. Chatrchyan *et al.* [CMS Collaboration], *Phys. Lett. B* **716**, 30-61 (2012).
- [3] G. Aad *et al.* [ATLAS Collaboration], *Eur. Phys. J. C* **76**, 658 (2016).
- [4] G. Aad *et al.* [ATLAS Collaboration], *Phys. Lett. B* **805**, 135426 (2020).
- [5] G. Aad *et al.* [ATLAS Collaboration], *Phys. Rev. Lett.* **125**, 061802 (2020).
- [6] A. M. Sirunyan *et al.* [CMS Collaboration], *Phys. Rev. Lett.* **125**, 061801 (2020).

- [7] A. Tumasyan *et al.* [CMS Collaboration], *JHEP* **06**, 012 (2022).
- [8] G. Steigman, *Ann. Rev. Astron. Astrophys.* **14**, 339-372 (1976).
- [9] A. G. Cohen and D. B. Kaplan, *Phys. Lett. B* **199**, 251-258 (1987).
- [10] G. Steigman, *JCAP* **10**, 001 (2008).
- [11] N. Cabibbo, *Phys. Rev. Lett.* **10**, 531 (1963).
- [12] M. Kobayashi and T. Maskawa, *Prog. Theor. Phys.* **49**, 652-657 (1973).
- [13] A. Riotto and M. Trodden, *Ann. Rev. Nucl. Part. Sci.* **49**, 35-75 (1999).
- [14] V. A. Kuzmin, V. A. Rubakov and M. E. Shaposhnikov, *Phys. Lett. B* **155**, 36 (1985).
- [15] G. F. Giudice, C. Grojean, A. Pomarol and R. Rattazzi, *JHEP* **06**, 045 (2007).
- [16] A. Alloul, B. Fuks and V. Sanz, *JHEP* **04**, 110 (2014).
- [17] J. Alwall, R. Frederix, S. Frixione, V. Hirschi, F. Maltoni, O. Mattelaer, H. S. Shao, T. Stelzer, P. Torrielli and M. Zaro, *JHEP* **07**, 079 (2014).
- [18] A. Alloul, N. D. Christensen, C. Degrande, C. Duhr and B. Fuks, *Comput. Phys. Commun.* **185**, 2250-2300 (2014).
- [19] C. Degrande, C. Duhr, B. Fuks, D. Grellscheid, O. Mattelaer and T. Reiter, *Comput. Phys. Commun.* **183**, 1201-1214 (2012).
- [20] J. Ellis, V. Sanz and T. You, *JHEP* **03**, 157 (2015).
- [21] C. Englert, R. Kogler, H. Schulz and M. Spannowsky, *Eur. Phys. J. C* **76**, 393 (2016).
- [22] H. Khanpour, S. Khatibi and M. M. Najafabadi, *Phys. Lett. B* **773**, 462-469 (2017).
- [23] F. Ferreira, B. Fuks, V. Sanz and D. Sengupta, *Eur. Phys. J. C* **77**, 675 (2017).
- [24] H. Denizli, K. Y. Oyulmaz and A. Senol, *J. Phys. G: Nucl. Part. Phys.* **46**, 105007 (2019).
- [25] H. Denizli and A. Senol, *Acta Phys. Polon. B* **52**, 1377 (2021).
- [26] H. Denizli and A. Senol, *Nucl. Phys. B* **962**, 115274 (2021).
- [27] J. Ellis, V. Sanz and T. You, *JHEP* **07**, 036 (2014).
- [28] S. Kumar, P. Poulose and S. Sahoo, *Phys. Rev. D* **91**, 073016 (2015).
- [29] J. Ellis and T. You, *JHEP* **03**, 089 (2016).
- [30] H. Khanpour and M. M. Najafabadi, *Phys. Rev. D* **95**, 055026 (2017).
- [31] S. Alam, S. Behera, S. Kumar and S. Sahoo, *Int. J. Mod. Phys. A* **32**, 1750017 (2017).
- [32] J. Ellis, P. Roloff, V. Sanz and T. You, *JHEP* **05**, 096 (2017).
- [33] H. Denizli and A. Senol, *Adv. High Energy Phys.* **2018**, 1627051 (2018).
- [34] O. Karadeniz, A. Senol, K. Y. Oyulmaz and H. Denizli, *Eur. Phys. J. C* **80**, 229 (2020).

- [35] S. Kuday, H. Saygin, I. Hos and F. Cetin, *Nucl. Phys. B* **932**, 1-14 (2018).
- [36] H. Hesari, H. Khanpour and M. M. Najafabadi, *Phys. Rev. D* **97**, 095041 (2018).
- [37] S. Spor, *J. Phys. G: Nucl. Part. Phys.* **51**, 065003 (2024).
- [38] C. Accettura *et al.*, *Eur. Phys. J. C* **83**, 864 (2023).
- [39] G. Aad *et al.* [ATLAS Collaboration], *Phys. Lett. B* **753**, 69-85 (2016).
- [40] M. Aaboud *et al.* [ATLAS Collaboration], *Phys. Rev. D* **98**, 052005 (2018).
- [41] ATLAS Collaboration, “Measurements and interpretations of Higgs-boson fiducial cross sections in the diphoton decay channel using 139 fb^{-1} of pp collision data at $\sqrt{s} = 13 \text{ TeV}$ with the ATLAS detector,” ATLAS-CONF-2019-029 (2019).